Acta Neurochir (2010) 152:2029–2036
DOI 10.1007/s00701-010-0779-2

CLINICAL ARTICLE

Is MRI a reliable tool to locate the electrode after deep brain stimulation surgery? Comparison study of CT and MRI for the localization of electrodes after DBS

Ji Yeoun Lee · Jin Wook Kim · Jee-Young Lee · Yong Hoon Lim · Cheolyoung Kim · Dong Gyu Kim · Beom Seok Jeon · Sun Ha Paek

Received: 12 October 2009 / Accepted: 13 August 2010 / Published online: 30 September 2010

Abstract
Purpose MRI has been utilized to localize the electrode after deep brain stimulation, but its accuracy has been questioned due to image distortion. Under the hypothesis that MRI is not adequate for evaluation of electrode position after deep brain stimulation, this study is aimed at validating the accuracy of MRI in electrode localization in comparison with CT scan.

Methods Sixty one patients who had undergone STN DBS were enrolled for the analysis. Using mutual information technique, CT and MRI taken at 6 months after the operation were fused. The x and y coordinates of the centers of electrodes shown of CT and MRI were compared in the fused images to calculate average difference at five different levels. The difference of the tips of the electrodes, designated as the z coordinate, was also calculated.
Results The average of the distance between the centers of the electrodes in the five levels estimated in the fused image of brain CT and MRI taken at least 6 months after STN DBS was 1.33 mm (0.1–5.8 mm). The average discrepancy of x coordinates for all five levels between MRI and CT was 0.56±0.54 mm (0–5.7 mm), the discrepancy of y coordinates was 1.06±0.59 mm (0–3.5 mm), and for the z coordinate, it was 0.98±0.52 mm (0–3.1 mm) (all p values <0.001). Notably, the average discrepancy of x coordinates at 3.5 mm below AC–PC level, i.e., at the STN level between MRI and CT, was 0.59±0.42 mm (0–2.4 mm); the discrepancy of y coordinates was 0.81±0.47 mm (0–2.9 mm) (p values<0.001).
Conclusions The results suggest that there was significant discrepancy between the centers of electrodes estimated by CT and MRI after STN DBS surgery.

Keywords CT · DBS · Electrode localization · Image fusion · MRI · Parkinson's disease

J. Y. Lee · J. W. Kim · Y. H. Lim · D. G. Kim · S. H. Paek (✉)
Department of Neurosurgery,
Seoul National University College of Medicine,
28 Yeongeon-dong, Jongno-gu,
Seoul 110-744, South Korea
e-mail: paeksh@snu.ac.kr

J.-Y. Lee · B. S. Jeon (✉)
Department of Neurology,
Seoul National University College of Medicine,
28 Yeongeon-dong, Jongno-gu,
Seoul 110-744, South Korea
e-mail: brain@snu.ac.kr

S. H. Paek
Ischemic/Hypoxic Disease Institute,
Seoul National University College of Medicine,
Seoul, South Korea

S. H. Paek
Cancer Research Institute,
Seoul National University College of Medicine,
Seoul, South Korea

B. S. Jeon · S. H. Paek
Clinical Research Institute, Seoul National University Hospital,
Seoul, South Korea

C. Kim
Medical Imaging Laboratory, CyberMed, Inc.,
Seoul, South Korea

Introduction

Deep brain stimulation (DBS) of the subthalamic nucleus (STN) has been proven as effective for the management of the advanced Parkinson's disease (PD) patients treated with long-term use of anti-PD drugs [12, 13]. The accurate

targeting of STN during the operation is important for a good clinical outcome after STN DBS. Determining the location of the electrode is also important for the estimation of clinical outcome of the patients with advanced PD after STN DBS surgery [25, 28]. MRI has been frequently utilized to target the STN during the operation and estimate the DBS electrode positions after STN DBS in the literature [1, 2, 4, 5, 7, 16, 17, 19, 21, 22, 31, 34–37].

Although MRI is a good tool to visualize the anatomical details of the brain with good resolution, image distortion caused by the local magnetic field inhomogeneity of electrodes could be a concern for the accuracy of the MR images in the estimation of electrode position in the patients treated with STN DBS [21, 29].

In a recently published article, we have evaluated the usefulness of reprogramming guided by the fused images of MRI and CT in STN DBS of PD patients. Clinical improvement was clearly shown by comparing the patient outcomes before and after reprogramming [11]. Through this study, numerical data comparing the center of the electrodes estimated by MRI and CT taken at 6 months after STN DBS was evaluated to validate accuracy of MRI as a reliable tool to estimate the electrode position after STN DBS.

Patients and method

Among 91 patients who underwent DBS between March 2005 and October 2006, 61 patients who had taken both MRI and CT at least 6 months after bilateral STN DBS were enrolled for the analysis. Thirty patients were excluded from the study, 15 of them had diseases other than PD, such as essential tremor or dystonia, seven patients had no follow-up images, another five patients had taken follow-up images but the uppermost level for the analysis was not included, and three patients had not taken the postoperative MRI or CT. This study was reviewed and permitted by the Institutional Research Board of Seoul National University Hospital (SNUH IRB). Informed consent was received from the patients for the examination of postoperative MRI. Bilateral DBS was done in 52 patients and unilateral in nine patients. The quadripolar DBS electrode model 3389 (Medtronic Sofamor Danek, Minneapolis, MN, USA), with four platinum iridium cylindrical surfaces (1.27 mm in diameter and 1.5 mm in length and 0.5 mm center-to-center separation) and Soletra model 7428 implantable pulse generator (Medtronic Neurological Division, Minneapolis, MN, USA) were implanted in a single session.

On the day of the surgery, stereotactic MRI was performed for the patient with the Leksell G frame (Elekta Instruments AB, Stockholm, Sweden) on, which was applied under local anesthesia. The stereotactic MRI was a 1.5-tesla MR imaging system (General Electric Medical Systems, Milwaukee, WI, USA) using an eight-channel head coil with 2 mm contiguous axial proton density T2-weighted images and 1.5 mm interleaved contiguous axial T1-weighted images with and without contrast gadolinium enhancement. The MRI was performed with the same protocols as the preoperative MRI and 3D spiral brain CT (64-channel Brilliance CT, Philips, Eindhoven, the Netherlands) with a 1-mm slice thickness at least 6 months after STN DBS surgery. The MRI and CT scans were not performed on the same day.

Image fusion of MRI and CT scan taken at least 6 months after STN DBS surgery was performed by using mutual information technique previously described elsewhere [14]. We utilized the Lucion® software (Cybermed, Seoul, Korea) based on the Windows operating system allowing simultaneous movement of the cursor in 3D orthogonal planes. The T2-weighted axial images are fused with 3D spiral CT scan images at the data set of 1 mm thickness reformatted images, aligned to anterior commissure–posterior commissure (AC–PC) line. The midline of reformatted coronal images also intersects the midsagittal plane for the correction of head-rotation error.

On the reformatted axial view, the position of electrode center is localized as a dot by adjusting window level in CT scan. In contrast, on the brain MRI, the position of electrode center is estimated as an imaginary center of image artifact of the electrode caused by local magnetic field inhomogeneity. The distance between the center of the dot-like electrode in the brain CT and imaginary center of electrode artifact in the brain MRI was calculated as shown in Fig. 1. The x and y coordinates of the centers of electrodes in CT and MRI were compared to calculate the average discrepancy of electrode position estimated in CT/MRIs, and the z coordinates of the tips of the electrodes were also compared. Such measurement was done for five levels, 30 mm (centrum semiovale), 20 mm (corpus callosum), 10 mm (septum pellucidum) above the level of the AC–PC line, at the level of AC–PC line, and 3.5 mm below the level of AC–PC line (at the level of STN) considering the irregular contour of the electrode from proximal to distal causing the shape of the artifact on MRI different at each level, as shown in Fig. 2.

For all the measurements including the distance between the two centers and x, y coordinates, only the absolute values were recorded, meaning all measurements had a positive value. The directions of each coordinate were not considered since this study was intended to show the absolute length of difference between the two centers regardless of its direction.

To investigate the interobserver reliability, calculations were repeated by another engineer for all of the patients.

Statistical analysis

To assess the differences between the two kinds of imaging techniques, measurements of the x, y, and z coordinates at

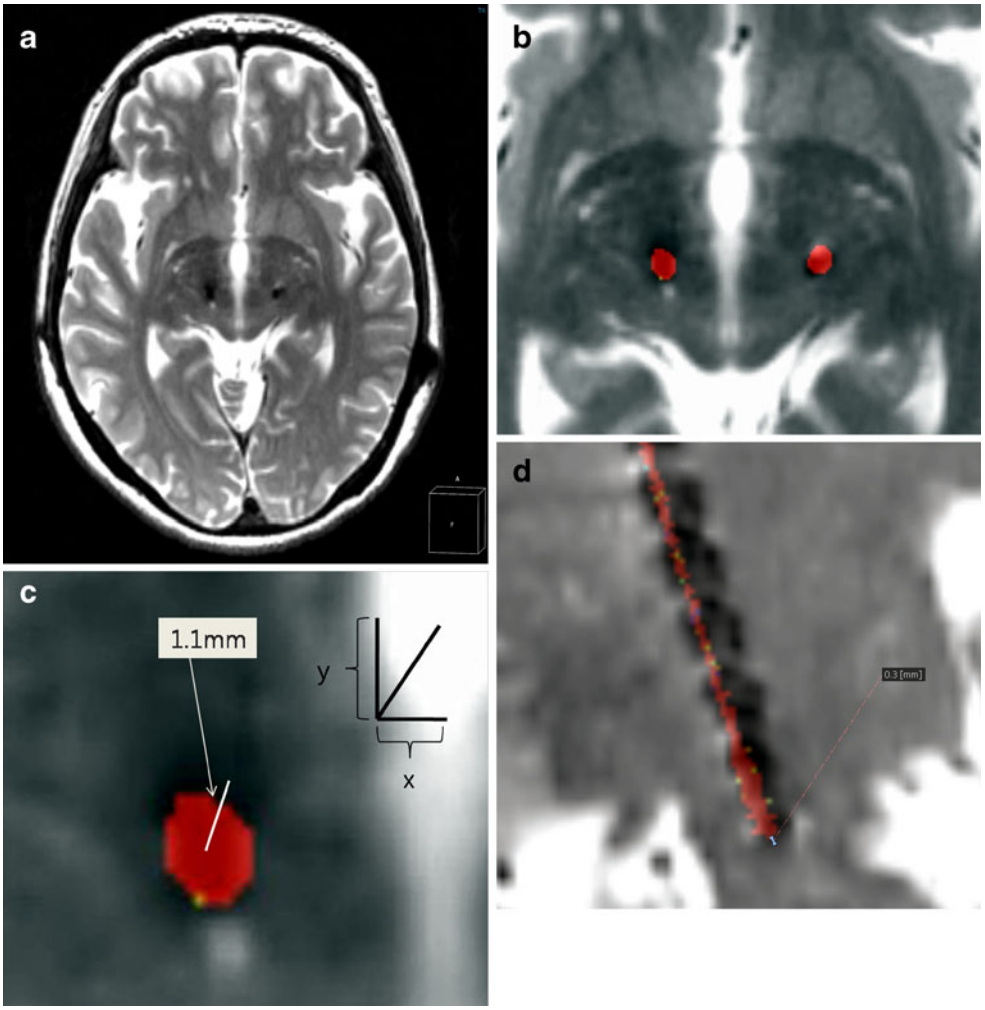

Fig. 1 Image fusion of brain CT and MRI taken at 6 months after STN DBS by using mutual information technique. The electrode is seen as an irregular round shape in the T2WI axial view at the STN level (3.5 mm below the AC–PC plane) (**a**). The electrode extracted from the CT is marked in *red spheres* in the axial view after fusion with MRI by using mutual information technique (**b**). The *white line* is connecting the center of the artifact on the MRI and CT. It is depicted as 1.1 mm, which is the distance between the center of the electrode on CT and MRI. The *inset* on the left upper corner shows the *x* and *y* values measured from the distance (**c**). The difference of the tip of electrode position is measured on the coronal plane as *z* coordinates (**d**)

each level were compared using the linear mixed model, allowing for correlations between measurements such as the level and laterality. Intraclass correlations (ICC) with 95% CI were obtained for two observers for interobserver reliability. Statistical significance was set at p value less than 0.05. All statistical analyses were performed using SPSS® ver 12.0 (SPSS, Chicago, IL, USA).

Results

The patients were 29 men and 32 women, with a mean age of 57.7 years (range: 26–73). A total of 113 electrodes were analyzed. All patients had follow-up images of MRI and CT, taken at least 6 months after the operation (range: 6–30 months, mean: 10.4 months).

Average distances between the center of electrodes shown on MRI and CT were 1.40±0.74 mm (0.2–5.8 mm) at 30 mm above the AC–PC plane, 1.35±0.65 mm (0.2–3.9 mm) at 20 mm above, 1.32±0.61 mm (0.1–3.6 mm) at 10 mm above, 1.31±0.59 mm (0.2–3.5 mm) at the level of AC–PC plane, and 1.08±0.47 mm (0.1–2.7 mm) at the level of STN, which was measured 3.5 mm below the AC–PC plane (Fig. 3). As explained before, for all the measurements, direction was not considered and the average of the absolute values was calculated. The values for x, y, z coordinates for the five levels are listed in Table 1. Statistic analysis showed significant difference in the x, y coordinates of all five levels and z coordinates ($p<0.001$).

The two-reader interobserver ICC was not high, 0.45 (95% CI) (0.35 to 0.54). The average distance for each level, as measured by the second reader, is shown in Table 2.

Discussion

In this study, we found that the direct fusion of brain MRI and brain CT scan taken at 6 months after STN DBS revealed a significant discrepancy of the centers of electrodes estimated by each modality. The method of evaluation in this study is different from the previous reports in that

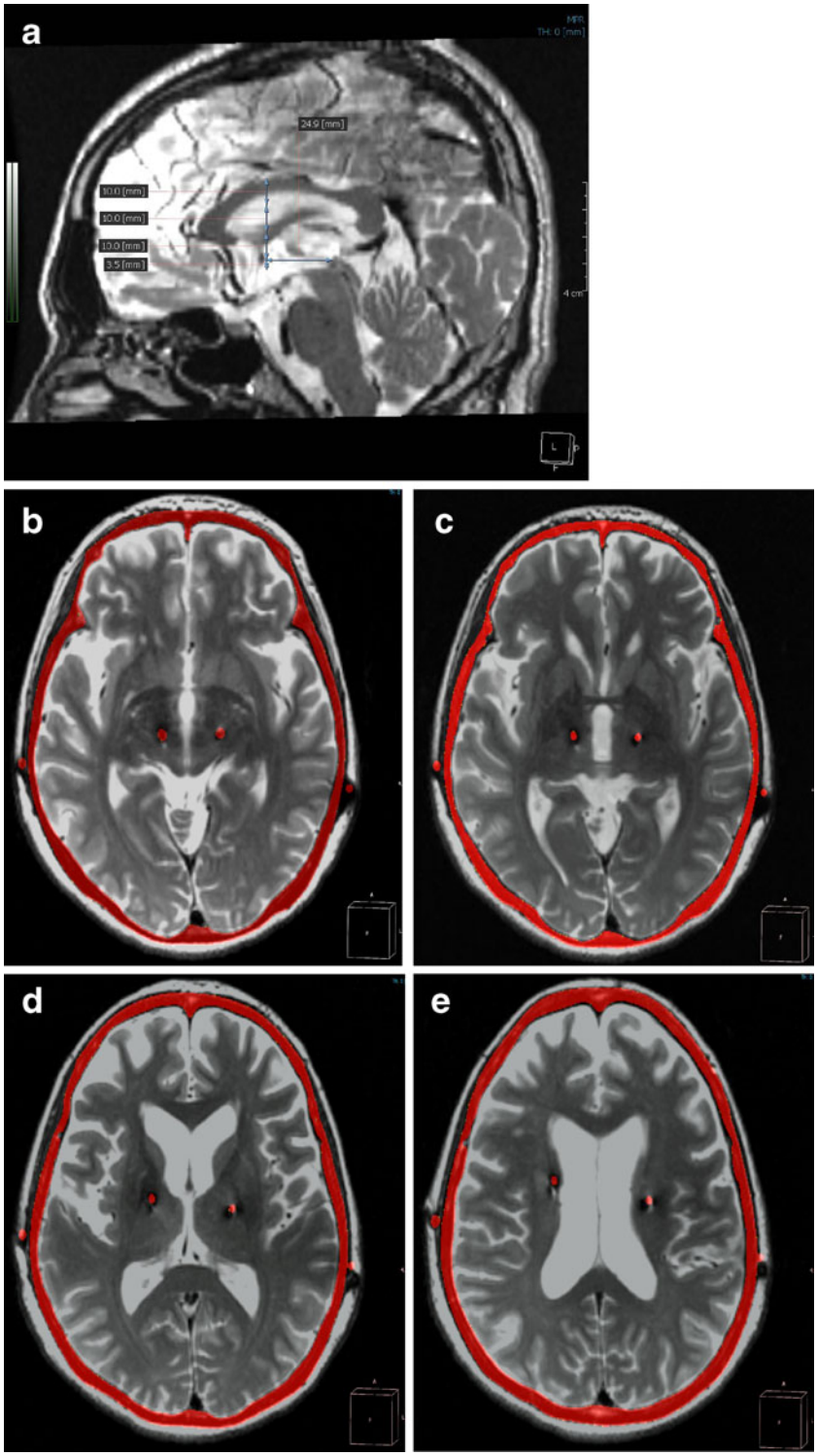

Fig. 2 Visualization of electrodes in the fused image of brain CT and MRI. T2WI sagittal view showing the AC–PC line (*horizontal blue line*), and the five levels are marked in *vertical blue lines* (**a**). At the lowest level, 3.5 mm below the AC–PC line, the STN is well visualized along with the red nucleus and putamen (**b**). At the level of the AC–PC line, putamen is usually seen in this level (**c**). At the level 10 mm above the AC–PC line, the septum pellucidum, thalamus, and the caudate nucleus, third ventricle, fornix are well visualized (**d**). At 20 mm above the AC–PC line, where the corpus callosum, caudate nucleus, and lateral ventricles are usually visible (**e**)

direct comparison of the centers of electrodes estimated on MRI and CT was performed instead of comparing the specific anatomical landmarks, such as AC or PC.

Despite the wide use of MRI in stereotactic neurosurgical procedures, the distortion of normal anatomical structures in MRI was questioned in comparison with brain CT scans. Such studies focused on the reliability of MRI in target localization. Such reports concluded that, though some differences were identified, they were not significant and that MRI alone may be used for target localization [8, 9].

Relatively less attention has been paid to the accuracy of MRI in localization of the electrode, and the results have

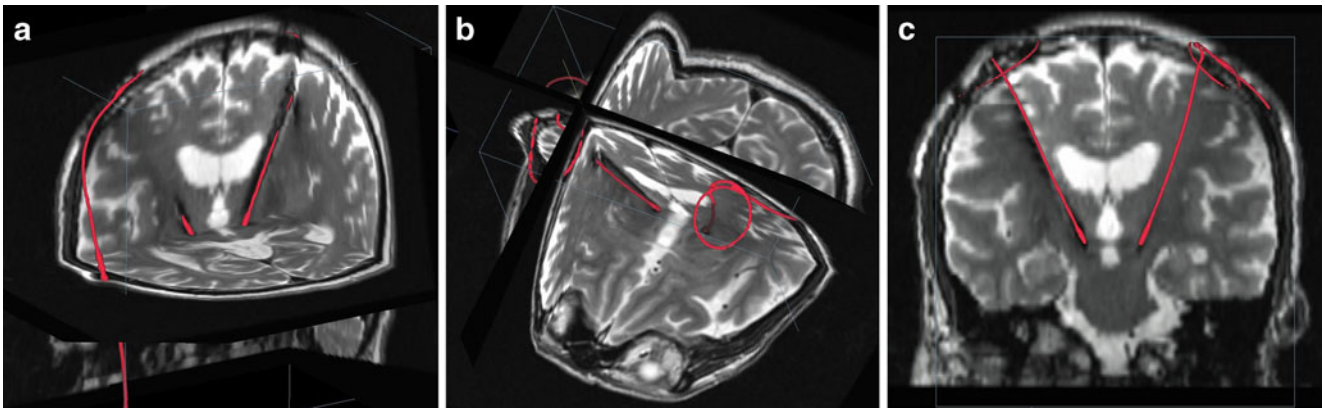

Fig. 3 3D visualization of electrodes in the fused image of brain CT and MRI. The electrodes on CT have been reconstructed and are shown as the *red lines* and fused onto the MRI images and visualized in 3D. Coronal cut viewed from anterior (**a**), from above (**b**) and from oblique position (**c**); all clearly show the discrepancy of the *red line* and the *blurry black line*, which is how the electrode is shown on MRI

been controversial. In one phantom study, in vitro and in vivo lengths between the proximal and distal end of the electrode contacts were measured and compared [20]. They concluded that the center of the artifact was concordant with the actual center of the electrode. A recent study comparing ventriculography and MRI also suggested that it was not crucial for electrode contact localization, though there was a translation of the electrode location induced by MRI scanning [5].

However, another study showed, by calculating the magnetic field perturbations using a Fourier-based method for various wire microelectrodes, that significant amount of artifact is produced depending on the magnetic susceptibility of the material used, the size, shape, and orientation of the electrodes with respect to the main magnetic field [15]. They concluded that the platinum–iridium microwire, commonly used for DBS, shows a complete signal loss that covers a volume 400 times larger than the actual volume occupied by the microelectrode [15].

The results of this study showed there was, in average, a 1.33-mm difference (0.1–5.8 mm) between the electrodes in the fused images of the MRI and CT by using mutual information technique. At the level of the STN, the average of difference between the electrode on the CT and the center on the MRI was 1.08 mm (0.1–2.7 mm). At the level of the STN (3.5 mm below the AC–PC plane), it was hard to delineate the center of the MRI artifact, since, on T2WI the STN had low signal, as well as the artifact. The range of

Table 1 Linear mixed model analysis for distance, *x*, *y*, *z* coordinates between the center of electrode on CT and MRI for five different levels

	Level	Average±SD (mm)	Range (mm)	*p* value
D	30 mm above AC–PC plane	1.40±0.74	0.2–5.8	<0.001
	20 mm above AC–PC plane	1.35±0.65	0.2–3.9	<0.001
	10 mm above AC–PC plane	1.32±0.61	0.1–3.6	<0.001
	0 mm above AC–PC plane	1.31±0.59	0.2–3.5	<0.001
	3.5 mm below AC–PC plane	1.08±0.47	0.1–2.7	<0.001
x	30 mm above AC–PC plane	0.56±0.70	0–5.7	<0.001
	20 mm above AC–PC plane	0.54±0.56	0–3.9	<0.001
	10 mm above AC–PC plane	0.52±0.47	0–2.1	<0.001
	0 mm above AC–PC plane	0.57±0.51	0–2.9	<0.001
	3.5 mm below AC–PC plane	0.59±0.42	0–2.4	<0.001
y	30 mm above AC–PC plane	1.14±0.59	0–3.0	<0.001
	20 mm above AC–PC plane	1.14±0.61	0–3.5	<0.001
	10 mm above AC–PC plane	1.13±0.60	0–3.5	<0.001
	0 mm above AC–PC plane	1.07±0.58	0–2.9	<0.001
	3.5 mm below AC–PC plane	0.81±0.47	0–2.9	<0.001
z		0.98±0.52	0–3.1	<0.001

D distance

Table 2 Distance calculated by two different raters at five levels

Level	D (1st reader) (mm)	D (2nd reader) (mm)
30 mm above AC–PC plane	1.40±0.74	0.95±0.50
20 mm above AC–PC plane	1.35±0.65	1.00±0.52
10 mm above AC–PC plane	1.32±0.61	1.00±0.52
0 mm above AC–PC plane	1.31±0.59	0.93±0.51
3.5 mm below AC–PC plane	1.08±0.47	0.80±0.33

D distance

measurement was wide, from 0.2 to 5.8 mm. Such results suggest the variability and inconsistency in the estimation of the electrode position based on the MRI compared to CT.

Such inconsistent estimation was also suggested by how the shape of the artifact varied on each level, making it difficult to decide where the center of the artifact was. For example, in one level, it looked like a round sphere, where as in another level, the same electrode had the appearance of a figure of eight (Fig. 2). The difference can be explained by the angle in which the electrode is placed in relation to the magnetic field in the MR instrument, since the electrode causing local magnetic inhomogeneity is not parallel but in a slanted angle in reference to the axis of the magnetic field. The discrepancy between CT and MRI can be clearly visualized on the 3D reconstructed, fused images of the two modalities (Fig. 3). Another point in inconsistent estimation is shown by the low ICC, meaning the measurements were variable when a different observer performed the measurements. We saw that the major component of this "unreliability" came from the fact that, due to such variable shape of the electrode on the MRI, the center could not be defined without variation. Though the measurements were not reliable, the discrepancy between the center of electrodes on MRI and CT is repetitively shown in the measurements of the second observer, as in Table 1. The average distance is about 1 mm in all levels.

To our knowledge, this is the first attempt of direct comparison of the location of the center of DBS electrodes estimated in the brain CT and MRI by using mutual information technique. The supposed center estimated based on the brain MRI is too variable to count on for accurate estimation of position of electrodes in relation to deep brain structures such as STN. Thus, we suggest that using postoperative brain CT in fusion with preoperative brain MRI is better for the accurate localization of STN DBS electrodes with surrounding anatomical details in the patients treated with STN DBS surgeries.

In taking the MR images of the patients with advanced PD several months after STN DBS, the safety issue is another concern in terms of local heating of the electrode located in the deep brain by RF pulse during the MRI scanning. With this study, the safety issue of brain MRI in the patients treated with STN DBS is worthy of note again. The public health notification issued on May 10, 2005 by the Food and Drug Administration (FDA) of the USA was sent to neuro-radiologists all over the world. It notified that the FDA had received several reports of serious injury, including coma and permanent neurological impairment, in patients with implanted neurological stimulators who underwent MRI procedures. However, there have been numerous reports in which careful following of the guidelines provided by the manufacturer resulted in safe performance of MRI in patients with neurostimulator electrodes implanted [3, 6, 23, 24, 26, 27, 32, 33, 38]. A recent report also summarized the complications after 3,304 PD patients underwent MRI after electrode insertion, which revealed just one IPG failure without neurological sequelae [30]. We previously reported our results regarding examination of brain MRI in the advanced PD patients treated with STN DBS [10, 18]. Along with the same protocol taken in the previous report, this study mostly had followed the guidelines from the manufacturers, except the notification of SAR, which was 0.1 W/kg or less. Nevertheless, none of the patients experienced any adverse effects in performing the postoperative 1.5-T brain MRIs taken 6 months later. Out of the 61 patients, six patients had taken lumbar spine MRIs after the operation. Though the manufactures had not set guidelines for MRIs other than brain MRI, we got informed consent and permission for lumbar spine MRI also. We had set the stimulation setting to the default values before taking the MRI, and then reset it back to the patient's settings. No patient experienced any discomfort or complications after the MRI.

The limitation of this study is that it lacks correlation with clinical outcome. The significance of "1 mm" would be accepted only with clear difference in the surgical outcome of the patients. We would like to point out that, although statistically significant inaccuracy of MRI was shown, this does not mean that all the previous clinical practices or studies using MRI were inaccurate. Indeed, we have published a paper evaluating the clinical outcome in relation to the accuracy of insertion of electrode into the target [18]. We have used the "incorrect" modality of MRI in evaluating the electrode position. Additionally, we also recently published another paper on reprogramming results using the rather "correct" modality of postoperative CT in the same group of patients [11]. We have noted in general that the clinical outcome was not much different. Therefore, the conventional method of using MRI as a tool that may have a significant error of "1 mm" may be tolerated for the majority of the patients. The clinical significance of "1 mm" may be found in cases where the electrode is positioned at the margin of the target. In such cases, the position of the electrode may be inaccurately assessed as

being "inside the target" when it is actually "off the target." Then the patient with poor outcome may lose the chance of reprogramming or even repositioning of the electrode and be regarded as having "unexplained" poor outcome.

Conclusion

Our findings suggest that the electrode location evaluated by postoperative MRI may have significant discrepancy with the location estimated by brain CT scan. To localize the electrode position in relation with the deep brain structures, such as STN after surgery, a fusion of the preoperative MRI and postoperative CT may help the physicians by providing ease and confidence for postoperative assessments, such as reprogramming of stimulation parameters.

Acknowledgements This study was supported by a grant of the Korea Healthcare technology R&D Project, Ministry for Health, Welfare & Family Affairs, Republic of Korea (A092052).

Conflicts of interest None.

References

1. Bittar RG, Burn SC, Bain PG, Owen SL, Joint C, Shlugman D, Aziz TZ (2005) Deep brain stimulation for movement disorders and pain. J Clin Neurosci 12:457–463
2. Breit S, LeBas JF, Koudsie A, Schulz J, Benazzouz A, Pollak P, Benabid AL (2006) Pretargeting for the implantation of stimulation electrodes into the subthalamic nucleus: a comparative study of magnetic resonance imaging and ventriculography. Neurosurgery 58:ONS83–ONS95
3. Brooks ML, O'Connor MJ, Sperling MR, Mayer DP (1992) Magnetic resonance imaging in localization of EEG depth electrodes for seizure monitoring. Epilepsia 33:888–891
4. Counelis GJ, Simuni T, Forman MS, Jaggi JL, Trojanowski JQ, Baltuch GH (2003) Bilateral subthalamic nucleus deep brain stimulation for advanced PD: correlation of intraoperative MER and postoperative MRI with neuropathological findings. Mov Disord 18:1062–1065
5. Coyne T, Silburn P, Cook R, Silberstein P, Mellick G, Sinclair F, Fracchia G, Wasson D, Stanwell P (2006) Rapid subthalamic nucleus deep brain stimulation lead placement utilising CT/MRI fusion, microelectrode recording and test stimulation. Acta Neurochir Suppl 99:49–50
6. Dormont D, Cornu P, Pidoux B, Bonnet AM, Biondi A, Oppenheim C, Hasboun D, Damier P, Cuchet E, Philippon J, Agid Y, Marsault C (1997) Chronic thalamic stimulation with three-dimensional MR stereotactic guidance. AJNR Am J Neuroradiol 18:1093–1107
7. Hamel W, Fietzek U, Morsnowski A, Schrader B, Herzog J, Weinert D, Pfister G, Muller D, Volkmann J, Deuschl G, Mehdorn HM (2003) Deep brain stimulation of the subthalamic nucleus in Parkinson's disease: evaluation of active electrode contacts. J Neurol Neurosurg Psychiatry 74:1036–1046
8. Holtzheimer PE 3rd, Roberts DW, Darcey TM (1999) Magnetic resonance imaging versus computed tomography for target localization in functional stereotactic neurosurgery. Neurosurgery 45:290–297, discussion 297–298
9. Kondziolka D, Dempsey PK, Lunsford LD, Kestle JR, Dolan EJ, Kanal E, Tasker RR (1992) A comparison between magnetic resonance imaging and computed tomography for stereotactic coordinate determination. Neurosurgery 30:402–406, discussion 406–407
10. Lee JY, Han JH, Kim HJ, Jeon BS, Kim DG, Paek SH (2008) STN DBS of advanced Parkinson's disease experienced in a specialized monitoring unit with a prospective protocol. J Korean Neurosurg Soc 44:26–35
11. Lee JY, Jeon BS, Paek SH, Lim YH, Kim MR, Kim C (2010) Reprogramming guided by the fused images of MRI and CT in subthalamic nucleus stimulation in Parkinson disease. Clin Neurol Neurosurg 112:47–53
12. Limousin P, Krack P, Pollak P, Benazzouz A, Ardouin C, Hoffmann D, Benabid AL (1998) Electrical stimulation of the subthalamic nucleus in advanced Parkinson's disease. N Engl J Med 339:1105–1111
13. Limousin P, Pollak P, Benazzouz A, Hoffmann D, Le Bas JF, Broussolle E, Perret JE, Benabid AL (1995) Effect of parkinsonian signs and symptoms of bilateral subthalamic nucleus stimulation. Lancet 345:91–95
14. Maes F, Collignon A, Vandermeulen D, Marchal G, Suetens P (1997) Multimodality image registration by maximization of mutual information. IEEE Trans Med Imaging 16:187–198
15. Martinez-Santiesteban FM, Swanson SD, Noll DC, Anderson DJ (2007) Magnetic field perturbation of neural recording and stimulating microelectrodes. Phys Med Biol 52:2073–2088
16. McClelland S 3rd, Ford B, Senatus PB, Winfield LM, Du YE, Pullman SL, Yu Q, Frucht SJ, McKhann GM 2nd, Goodman RR (2005) Subthalamic stimulation for Parkinson disease: determination of electrode location necessary for clinical efficacy. Neurosurg Focus 19:E12
17. McClelland S 3rd, Senatus PB, Ford B, McKhann GM 2nd, Goodman RR (2007) Staged bilateral thalamic electrode implantation utilizing frameless stereotactic guidance. J Clin Neurosci 14:791–793
18. Paek SH, Han JH, Lee JY, Kim C, Jeon BS, Kim DG (2008) Electrode position determined by fused images of preoperative and postoperative magnetic resonance imaging and surgical outcome after subthalamic nucleus deep brain stimulation. Neurosurgery 63:925–936, discussion 936–927
19. Pinto S, Le Bas JF, Castana L, Krack P, Pollak P, Benabid AL (2007) Comparison of two techniques to postoperatively localize the electrode contacts used for subthalamic nucleus stimulation. Neurosurgery 60:285–292, discussion 292–284
20. Pollo C, Villemure JG, Vingerhoets F, Ghika J, Maeder P, Meuli R (2004) Magnetic resonance artifact induced by the electrode Activa 3389: an in vitro and in vivo study. Acta Neurochir (Wien) 146:161–164
21. Pollo C, Vingerhoets F, Pralong E, Ghika J, Maeder P, Meuli R, Thiran JP, Villemure JG (2007) Localization of electrodes in the subthalamic nucleus on magnetic resonance imaging. J Neurosurg 106:36–44
22. Rampini PM, Locatelli M, Alimehmeti R, Tamma F, Caputo E, Priori A, Pesenti A, Rohr M, Egidi M (2003) Multiple sequential image-fusion and direct MRI localisation of the subthalamic nucleus for deep brain stimulation. J Neurosurg Sci 47:33–39
23. Rezai AR, Lozano AM, Crawley AP, Joy ML, Davis KD, Kwan CL, Dostrovsky JO, Tasker RR, Mikulis DJ (1999) Thalamic stimulation and functional magnetic resonance imaging: localization of cortical and subcortical activation with implanted electrodes. Technical note. J Neurosurg 90:583–590
24. Rezai AR, Phillips M, Baker KB, Sharan AD, Nyenhuis J, Tkach J, Henderson J, Shellock FG (2004) Neurostimulation system used for deep brain stimulation (DBS): MR safety issues and implications of failing to follow safety recommendations. Invest Radiol 39:300–303

25. Saint-Cyr JA, Hoque T, Pereira LC, Dostrovsky JO, Hutchison WD, Mikulis DJ, Abosch A, Sime E, Lang AE, Lozano AM (2002) Localization of clinically effective stimulating electrodes in the human subthalamic nucleus on magnetic resonance imaging. J Neurosurg 97:1152–1166
26. Simon SL, Douglas P, Baltuch GH, Jaggi JL (2005) Error analysis of MRI and leksell stereotactic frame target localization in deep brain stimulation surgery. Stereotact Funct Neurosurg 83:1–5
27. Spiegel J, Fuss G, Backens M, Reith W, Magnus T, Becker G, Moringlane JR, Dillmann U (2003) Transient dystonia following magnetic resonance imaging in a patient with deep brain stimulation electrodes for the treatment of Parkinson disease. Case report. J Neurosurg 99:772–774
28. Starr PA, Vitek JL, Bakay RA (1998) Ablative surgery and deep brain stimulation for Parkinson's disease. Neurosurgery 43:989–1013, discussion 1013–1015
29. Sumanaweera TS, Adler JR Jr, Napel S, Glover GH (1994) Characterization of spatial distortion in magnetic resonance imaging and its implications for stereotactic surgery. Neurosurgery 35:696–703, discussion 703–694
30. Tagliati M, Jankovic J, Pagan F, Susatia F, Isaias IU, Okun MS, Grp NPFDW (2009) Safety of MRI in patients with implanted deep brain stimulation devices. Neuroimage 47:T53–T57
31. Tisch S, Zrinzo L, Limousin P, Bhatia KP, Quinn N, Ashkan K, Hariz M (2007) Effect of electrode contact location on clinical efficacy of pallidal deep brain stimulation in primary generalised dystonia. J Neurol Neurosurg Psychiatry 78:1314–1319
32. Tronnier VM, Staubert A, Hahnel S, Sarem-Aslani A (1999) Magnetic resonance imaging with implanted neurostimulators: an in vitro and in vivo study. Neurosurgery 44:118–125
33. Uitti RJ, Tsuboi Y, Pooley RA, Putzke JD, Turk MF, Wszolek ZK, Witte RJ, Wharen RE Jr (2002) Magnetic resonance imaging and deep brain stimulation. Neurosurgery 51:1423–1428, discussion 1428–1431
34. Vergani F, Landi A, Antonini A, Parolin M, Cilia R, Grimaldi M, Ferrarese C, Gaini SM, Sganzerla EP (2007) Anatomical identification of active contacts in subthalamic deep brain stimulation. Surg Neurol 67:140–146, discussion 146–147
35. Voges J, Volkmann J, Allert N, Lehrke R, Koulousakis A, Freund HJ, Sturm V (2002) Bilateral high-frequency stimulation in the subthalamic nucleus for the treatment of Parkinson disease: correlation of therapeutic effect with anatomical electrode position. J Neurosurg 96:269–279
36. Winkler D, Tittgemeyer M, Schwarz J, Preul C, Strecker K, Meixensberger J (2005) The first evaluation of brain shift during functional neurosurgery by deformation field analysis. J Neurol Neurosurg Psychiatry 76:1161–1163
37. Yelnik J, Damier P, Demeret S, Gervais D, Bardinet E, Bejjani BP, Francois C, Houeto JL, Arnule I, Dormont D, Galanaud D, Pidoux B, Cornu P, Agid Y (2003) Localization of stimulating electrodes in patients with Parkinson disease by using a three-dimensional atlas-magnetic resonance imaging coregistration method. J Neurosurg 99:89–99
38. Zhang J, Wilson CL, Levesque MF, Behnke EJ, Lufkin RB (1993) Temperature changes in nickel-chromium intracranial depth electrodes during MR scanning. AJNR Am J Neuroradiol 14:497–500